

Contextual amino acids required for N-terminal cysteine palmitoylation of $G\alpha q$

Maya Nakano

Department of Biology
The University of North Carolina Asheville
One University Heights
Asheville, North Carolina 28804 USA

Faculty Mentor: Dr. Thomas E. Meigs

Abstract

Heterotrimeric guanine nucleotide-binding proteins (G proteins) of the $G\alpha 12/13$ and $G\alpha q/11$ subfamilies are broadly implicated in cancerous signaling and tumor progression. The primary goal of this study was to understand the amino acid structures within these G proteins that target them for palmitoylation, a lipid modification required for many of their intracellular functions. Cancerous signaling by G proteins requires the enzymatic attachment of the fatty acid palmitate to cysteine amino acids located in their N-terminal regions. Although the role of cysteines as attachment points for lipids is well established, little is known about the role of other, adjacent amino acids in G proteins to allow their recognition by palmitoyl transferase enzymes. A primary question is whether differences in these flanking amino acids bestow different mechanisms of lipid attachment upon different G proteins, such as $G\alpha q$ vs. $G\alpha 12/13$. Engineering a “chimeric” $G\alpha 13$ containing the N-terminal amino acids of $G\alpha q$ will allow for the use of a $G\alpha 13$ -driven oncogenic pathway in cells to study the effects of manipulating $G\alpha q$ -specific amino acids. Results from these experiments showed that mutating N-terminal cysteines of $G\alpha 13$, $G\alpha q$, or their chimera fully abolished cancerous signaling, and mutations adjacent to these amino acids had varying effects on this function. In subsequent experiments, additional lipidation sites were engineered in these proteins to assess their ability to “rescue” cancerous signaling that had been lost in these proteins by Cys mutation. Early results suggest that $G\alpha 13$ and $G\alpha q$ have different lipid modification requirements. These findings will aid the development of inhibitory compounds that disrupt lipid attachment to specific G proteins in selected tumor types.

Introduction

Heterotrimeric G proteins are a critical class of molecules that convey external cellular signals to the cell interior and into intracellular responses. These proteins are comprised of three distinct subunits: $G\alpha$, $G\beta$, and $G\gamma$. Based on the sequence homology, the $G\alpha$ subunit is further categorized into four subfamilies: Gs, Gi, Gq/11, and G12/13. The activation of heterotrimeric G proteins is primarily mediated by G-protein-coupled receptors (GPCRs), which are located on the cell membrane and are stimulated by a diverse range of extracellular signaling molecules, such as hormones and neurotransmitters.

Functionally, G proteins act as molecular switches within the cell. In their inactive state, the three subunits remain associated, with $G\alpha$ bound to guanosine diphosphate (GDP). Activation of the G protein is facilitated by ligand binding to the GPCR, allowing for the release of GDP on the $G\alpha$ subunit in exchange for the binding of the more abundant guanosine triphosphate (GTP). This exchange induces a conformational change resulting in the $G\alpha$ subunit seeing a loss of affinity and subsequent dissociation from the $G\beta\gamma$ dimer, allowing both to independently regulate downstream signaling pathways that result in cell proliferation and cytoskeletal rearrangements (Wedegaertner, 2012).

G proteins have attracted attention in both cell biology and medical fields due to their role in tumorigenesis, with mutations in G proteins or their associated GPCRs identified in >20% of human tumors (Arang & Gutkind, 2020). In particular, $G\alpha_{12/13}$ and $G\alpha_{q/11}$ are implicated due to their regulatory functions in cell proliferation, and the capacity to impart hallmark oncogenic characteristics to cells (Arang & Gutkind, 2020, Rasheed et al., 2018, Rasheed et al., 2022). Under normal physiological conditions, wild type $G\alpha$ proteins maintain intrinsic GTPase activity, allowing for the hydrolysis of the bound GTP to GDP, switching the protein to an inactive state. However, specific mutations can end in GTPase deficiency, resulting in the persistent activation of the $G\alpha$ protein. Often, this is due to a key glutamine to leucine mutation, with the resulting $G\alpha$ protein denoted as a QL variant. While these GTPase-deficient mutations have been heavily implicated in the oncogenic signaling in many $G\alpha$ subunits, they are rarely observed in $G\alpha_{12/13}$ in human tumors. Aberrant signaling in the $G\alpha_{12/13}$ subfamily appears to predominantly stem from its overexpression, often seen without the presence of a GTPase-deficient mutation, with $G\alpha_{12/13}$ seeing a notable delay in GTP hydrolysis, keeping the active state protein signaling for longer (Hasan et al., 2023, Suzuki et al., 2009).

Comparatively, typical presentation within $G\alpha_{q/11}$ correlated cancers differs. Although $G\alpha_{q/11}$ shares an intrinsically decreased rate of GTP hydrolysis in wild-type condition, the presence of mutated GTPase-deficient $G\alpha_{q/11}$ is found in >90% of uveal melanoma cases, and tumorigenic in nude mice studies, strongly cementing it as an oncogenic driver once mutated (Arang & Gutkind, 2020., Annala et al., 2019). This suggests that while key similarities may be present between different $G\alpha$ subfamilies, the observable differences in aberrant signaling patterns point to critical mechanisms that drive cancerous signaling, either by the roles of contextual residues, signaling pathways, or enzymatic attachment.

$G_{\alpha 12/13}$ and $G_{\alpha q/11}$ promote cellular growth and proliferation by regulating the serum response element (SRE) growth signaling pathway, which results in the binding of the serum response factor (SRF) to the serum response element sequence found at SRE-regulated gene promoter sites. A signaling pathway leading to SRF activation is the Rho-mediated pathway utilised by both $G_{\alpha 12/13}$ and $G_{\alpha q/11}$. Notably, $G_{\alpha 12/13}$ and $G_{\alpha q/11}$ activate this pathway by different mechanisms and stimulation of different proteins. GTP-activated $G_{\alpha 12/13}$ and $G_{\alpha q/11}$ proteins activate the translocation of different Rho guanine nucleotide exchange factors (RhoGEFs) to the inner face of the plasma membrane, allowing the downstream stimulation of RhoA (Figure 1). $G_{\alpha 12/13}$ utilizes PDZ RhoGEF, Leukemia Associated RhoGEF (LARG), and P115 RhoGEF (Siehl, 2009). $G_{\alpha q/11}$ mobilizes TRIO and P63 RhoGEF to interact with RhoA (Maziarz et al, 2018). RhoA, once activated, induces the nuclear translocation of myocardin-related transcription factor A (MRTF-A), allowing it to form a complex with SRF as a coactivator for the SRE site and drive transcription of SRE-regulated genes (Hill et al., 1995, Yu & Brown, 2015).

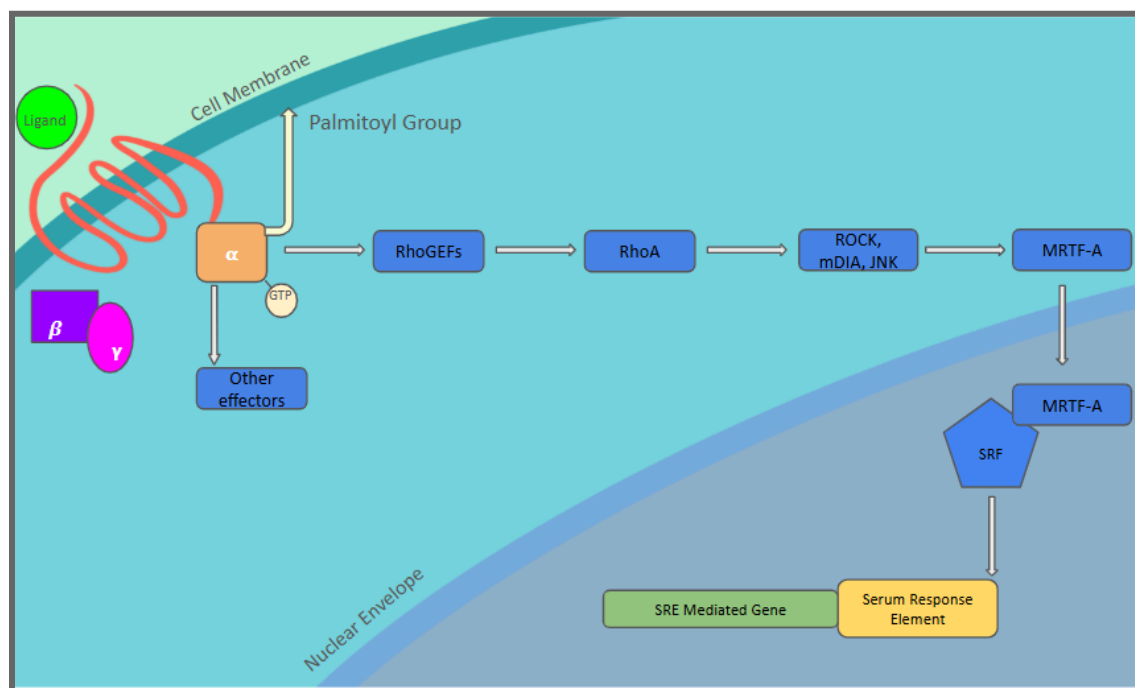


Figure 1. Above is the serum response factor (SRF) signaling pathway. Upon stimulation of the GPCR (red) by an extracellular ligand (light green circle), the $G_{\alpha q}$ subunit sees guanine nucleotide exchange, in which GDP is swapped for GTP, and the dissociation from $\beta\gamma$ dimer (purple and pink) occurs. Anchored to the membrane by a palmitoyl lipid group (light yellow), $G_{\alpha q}$ mobilizes TRIO and P63 RhoGEFs to interact with RhoA. RhoA, through a series of downstream effectors, allows for the nuclear translocation of MRTF-A, which forms a complex with SRF (dark yellow) to drive the transcription of SRE-regulated genes (dark green).

G protein signaling function, including by the $G_{\alpha 12/13}$ and $G_{\alpha q/11}$ subfamilies, requires covalent lipid attachment near the N-terminus; this modification appears to be important for correct membrane targeting and possibly protein interaction involving the

activated $G\alpha$ subunits. G proteins are predominantly localized to the inner surface of the cell membrane, and this dynamic placement is integral to their role in driving both regulatory and oncogenic signaling pathways (Wedegaertner, 2012). A key component governing this localization of G proteins is the enzyme that attaches the lipid, which for most $G\alpha$ subunits is a 16-carbon saturated fatty acid termed palmitate (Veit, et al., 1994). The class of enzymes implicated in this enzymatic lipid attachment includes the 23 members of the zDHHC family. It is not known which specific zDHHC enzymes target the $G\alpha12/13$ and $G\alpha q/11$ subfamilies (Qian, et al., 2025).

Previous studies have determined that mutating the N-terminal cysteine of several $G\alpha$ subunits prevents their signaling function, presumably by disrupting the palmitoyltransferase enzyme from attaching a lipid to the target cysteine (Bhattacharyya & Wedegaertner, 2000). However, the surrounding amino acid context of this cysteine in terms of targeting by the zDHHC enzyme is not well understood. Previous research was conducted to determine the rescue of cysteine-knockout $G\alpha13$ in both wild-type and active forms by integration of an MGAGAS myristoylation site at the N-terminus or CAAX isoprenyl lipid motif at the C-terminus. Constitutively-active $G\alpha13$ saw full rescue and upregulation of SRE signaling, while $G\alpha13$ -wt saw only rescue by isoprenyl lipid attachment, and not by myristoyl lipid attachment, suggesting a lipid specificity within the wild type that is lost in the mutated form (Hasan et al., 2023). This aberrant signaling correlated to contextual residues is further supported by research into $G\alpha12$. The N-terminal modification of the serine residue to the phosphomimic aspartic acid (Ser⁹ to Asp) disrupted the signaling of $G\alpha12$, as these phosphorylation sites allow for the activation of the GPCR (Chakravorty & Assmann, 2018). When the serine to aspartic acid mutation (Ser¹² to Asp) was conducted on $G\alpha13$, the signaling strength remained unaffected. To rescue the Ser-to-Asp mutant of $G\alpha12$ or the $G\alpha12$ -13 chimera, a myristoylation site was introduced at the extreme N-terminus, resulting in full signal rescue of both constructs (Cook, 2023).

With strong contextual assay data for $G\alpha12/13$ attachment and signaling and the effects of lipid attachment and serine involvement, $G\alpha q/11$ was chosen for study due to its structural and functional similarities with $G\alpha12/13$ to allow for comparative understanding of the effects of $G\alpha$ subunit signaling, lipid attachment specificity, and behavior. Thus, this study aims to further investigate the other families of $G\alpha$ subunits, specifically $G\alpha q/11$ through research of the contextual amino acids necessary (Figure 2) in the attachment of the palmitate lipid, and whether differences in these flanking residues provide different or similar signalling in response to phosphomimicry, localisation capability via modification of lipid sites and motifs to $G\alpha13$ -wt and constitutively-active $G\alpha13$, and establish comparative data between $G\alpha12/13$, and $G\alpha q/11$ subfamilies.

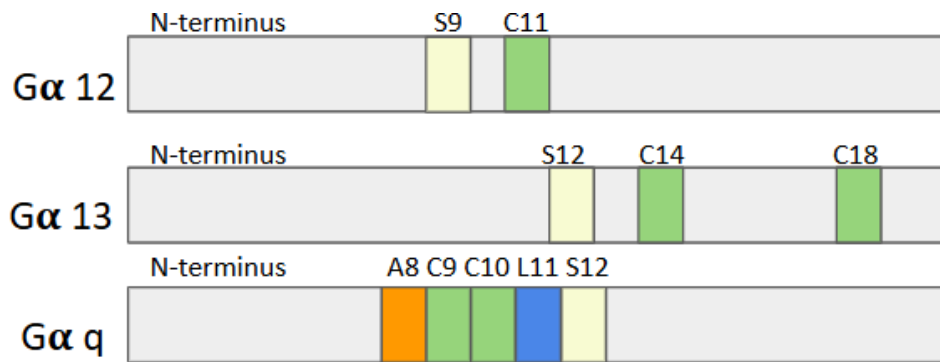


Figure 2. Sequence comparison of Gα12, Gα13, and Gαq highlighting key residues targeted for mutation to investigate the role of contextual residues on signaling strength. Mutations include the introduction of phosphomimicry, negative charges, and cysteine-knockout. The endogenous residues of interest are: Gα12-Ser⁹ and Cys¹¹; Gα13-Ser¹², Cys¹⁴, and Cys¹⁸; Gαq - Ala⁸, Cys⁹, Cys¹⁰, Leu¹¹, and Ser¹².

Materials and Methods

PCR-Derived Mutagenesis

All Gαq variants were engineered through polymerase chain reaction (PCR) mutagenesis, with initial fragments provided by Jack Hendrix (Meigs lab) created with intended modifications. The primary round of PCR saw the amplification of three Gαq oligos containing key point mutations. These fragments were then inserted into constitutively-active, where glutamine is replaced by leucine (Gln²⁰⁹ to Leu): Gαq-QL as a template sequence, and confirmed by gel electrophoresis. Purification of the constructs was performed via Wizard SV columns (Promega, Madison, WI) and subsequently digested utilizing KPN-HF and XHO-I (New England Biolabs, Ipswich, MA) enzymes and sites to isolate and clone into the vector plasmid PcDNA 3.1(+). The final plasmid sequences were confirmed (Genewiz, NJ) to determine the correct amplification and modification of Gαq/11. Subsequent constructs were similarly engineered through PCR and utilised constitutively-active Gαq and cysteine-knockout Gαq as template sequences.

Mammalian Cell Culture and Transfection

Human embryonic kidney (HEK293) cells were grown in Dulbecco's Modified Eagle's Media with 10% fetal bovine serum, and the cells were split after reaching confluence. Cells were then suspended using a 0.25% trypsin solution before being distributed equally among 12-well plates and incubated at 37 °C until cells reached ~80% confluence, visually determined by phase-contrast microscopy. Each well was transfected using 200 ng SRE-luciferase plasmid, 200 ng of construct-encoding plasmid, 10- 20 ng Renilla pRL-TK plasmid, and Gαq constructs, or pcDNA3.1(+).

Serum Response Element (SRE) Dual Firefly Luciferase Assays

Approximately 48 hours post-transfection, serum response element (SRE) luminometry assays were conducted to assess the signaling strength of constructs. Cells were washed in 1 mL 1x PBS and lysed with 250 μ L passive lysis buffer while under agitation at 120 rpm for 20 minutes to disrupt cells. Lysates were pelleted by centrifugation at 16,000 x g for 1 minute, and supernatants were collected for analysis. Dual-luciferase assays were performed using a GloMax 20/20 luminometer (Promega), with 40 μ L of supernatant mixed with 20 μ L of 4x/DTT to be saved for future SDS-Page and immunoblotting. Luminance was quantified in two steps: the first measurement was taken after catalysing the reaction of SRE-mediated firefly luciferase, which was followed by the quenching of the firefly luciferase reaction and stimulation of the Renilla luciferase. Firefly luciferase activity expression was measured as a representative of gross SRF activation by the SRE pathway, while Renilla luciferase activity, which is expressed independently, was subsequently measured to correct for variability in transfection efficiency. The resulting ratio of firefly luciferase to Renilla luciferase luminescence was interpreted as a quantitative measurement in representing the presence and strength of SRF pathway activation.

SDS-Page and Immunoblotting

To analyse protein expression, samples were subjected to sodium dodecyl sulfate polyacrylamide gel electrophoresis (SDS-Page) and immunoblotting. Lysate samples were denatured in 4x Laemmli buffer containing 0.1M dithiothreitol and SDS at 72° for approximately 10 minutes to ensure protein unfolding and run on a 12% polyacrylamide gel at 135 volts. After separation, the proteins were transferred onto a nitrocellulose membrane for immunoblotting by electroblotting. Blots were probed with anti-GNAQ (Proteintech, Rosemont, IL) or anti-GAPDH primary antibody (Abnova, Taipei City, Taiwan) mixed at a 1:2000 dilution within milk-TBST, followed by anti-rabbit and anti-mouse secondary antibodies (Promega). Detection and development of Western blots was done utilizing alkaline phosphatase, 5-bromo-4-chloro-3-indolyl phosphate (BCIP), and nitroblue tetrazolium (NBT). Imaging of the developed bands was done by use of a Kodak Gel Logic 100 system.

Results

Cystine to Alanine Mutations in $G\alpha_q$ Disrupt SRF Signaling, Serine to Aspartate and Phosphomimic Mutations Retain Signaling

To determine the role that N-terminal residues within $G\alpha_q$ play in signaling capability and test if the mechanism by which $G\alpha_q$ is palmitoylated is akin to that of $G\alpha_{12}$ or $G\alpha_{13}$, residues were subjected to point mutagenesis. Cysteine residues critical to palmitoylation were substituted with alanine (C9A, C10A) to preserve the hydrophobic

characteristic at this position while eliminating the thiol side chains of the cysteine residue (Figure 3). In addition, aspartic acid mutations mimicking constitutive phosphorylation (A8D, L11D, S12D) were generated to determine the effect of local N-terminal negative charges on signaling strength (Figure 3). The resulting mutants of constitutively-active $G\alpha_q$ -QL, C9A,C10A, A8D,L11D, and S12D were subjected to the luminometry assay, where measurement of luminance could be correlated to signaling strength, to determine if these mutations impacted their ability to signal through the SRF pathway. Alongside the constructs, $G\alpha_q$ -QL and vector PcDNA 3.1(+) were utilized as positive and negative controls, with luminance measurements of 417.05 ± 16.77 and 6.34 ± 0.40 , respectively (Figure 4). Consistent with previous studies on $G\alpha_{12/13}$, C9A,C10A failed to drive SRE signaling, measuring 6.56 ± 1.73 , matching the negative baseline control (Figure 4).

To investigate if phosphomimic modification would disrupt $G\alpha_q$ signaling strength, akin to those in previous studies on $G\alpha_{12}$, the double point mutant A8D,L11D, and single point mutant S12D were generated (Cook, 2022). In contrast to $G\alpha_{12}$, both A8D,L11D and S12D continued to signal, with luminescence values of 305.09 ± 47.88 and 348.34 ± 23.43 , respectively (Figure 4). After signaling strength was measured in all constructs, they were then immunoblotted to determine protein expression, to ensure that loss of signaling or expression was not from the absence of $G\alpha_q$ (Figure 4). These luminance and blotting results suggest that $G\alpha_q$ may utilize a different mechanism to drive lipid attachment, that, unlike $G\alpha_{12}$, remains functional despite the presence of phosphomimic residues.

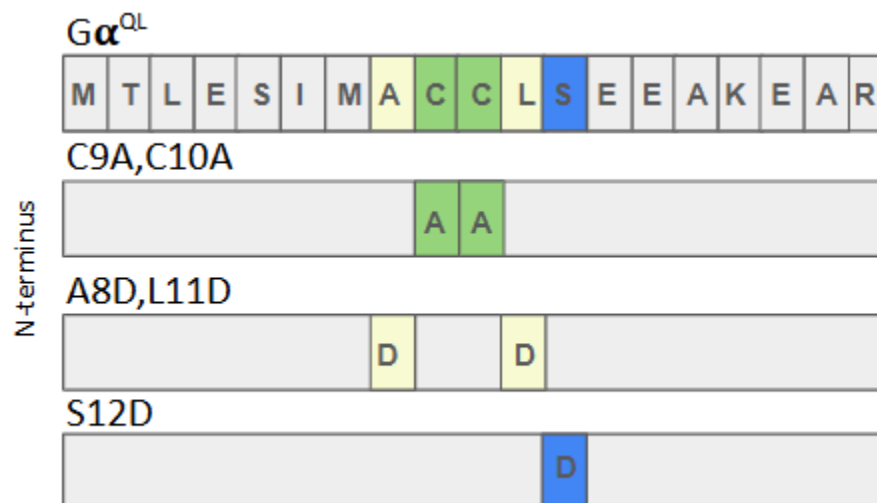


Figure 3. Sequence comparison of $G\alpha_q$ -QL highlighting key residues targeted for mutation to investigate the role of contextual residues on signaling strength. Mutations include constructs: C9A,C10A- Cys⁹, Cys¹⁰ to Ala, A8D,L11D- Ala⁸, Leu¹¹ to Asp, and S12D-Ser¹² to Asp.

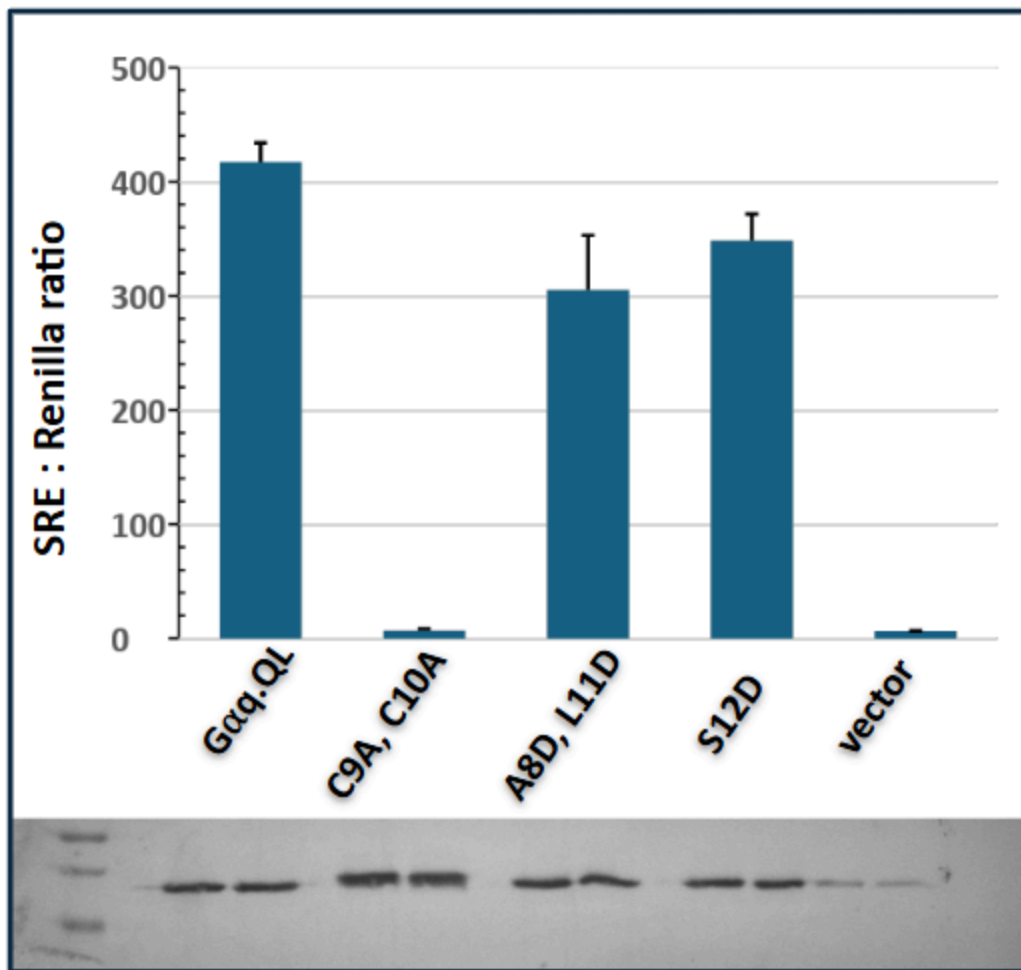


Figure 4. SRE signaling strength of GαqQL, pcDNA3.1(+) as controls, and mutants C9A,C10A, A8D,L11D, and S12D, as measured by luciferase assay (Methods 2.3). Values are representative of average signaling strength between replicates ± the range. Mutant C9A,C10A fails to signal, while A8D,L11D, and S12D mutants retain signaling capability. Expression of Gαq protein for all transfected samples was confirmed by western blot analysis, with two bands per sample in a replicate fashion. Bands representing Gαq-QL, C9A,C10A, A8D,L11D, and pcDNA3.1(+). Slight band presence seen in pcDNA3.1(+) represents endogenously-encoded Gαq.

Isoprenyl Lipid Attachment Fails to Rescue in Gαq Cys-to Ala Mutant

To investigate whether the loss of signaling in the C9A,C10A mutant was due to the absence of palmitoylation, and if this loss of signal could be rescued by alternative lipidation sites, constructs with previously investigated lipidation mechanisms were designed. The Gαq-QL and C9A,C10A sequences were modified to include an N-terminal myristoylation site (MGAGAS) or a C-terminal isoprenylation site (CAAX) to assess the effect on Gαq-QL, and the rescue potential within the cysteine-knockout

mutant of $G\alpha_q$ -QL (Figure 5). These modified constructs and controls: $G\alpha_q$ -QL, C9A,C10A, and vector pcDNA3.1(+) were subjected to SRE luminometry assays to quantify SRF growth pathway signaling. The control constructs $G\alpha_q$ -QL, C9A,C10A, and vector pcDNA3.1(+) were measured to have signaling levels of 796.48 +/- 306.26, 53.86 +/- 23.67, and 48.73 +/- 18.57 (Figure 6). With the addition of a myristoylation site (MGAGAS) at the N-terminus, the signal was significantly upregulated (Figure 6), measured at 1922.98 +/- 480.61. The introduction of the same MGAGAS site into the N-terminus of C9A,C10A mutant successfully restored SRF signaling, with results comparable to $G\alpha_q$ -QL, measured at 588.63 +/- 194.28 (Figure 6).

Subsequently, a C-terminal isoprenylation motif (CAAX) was introduced into constitutively-active $G\alpha_q$ to determine signaling strength. The resulting signal was measured at 849.56 +/- 232.21, a measurement akin to unmodified $G\alpha_q$ -QL. In contrast, when the CAAX motif was added to the C-terminal of the C9A,C10A mutant, no rescue of signaling was detected, measured at 41.01 +/- 23.67 (Figure 6).

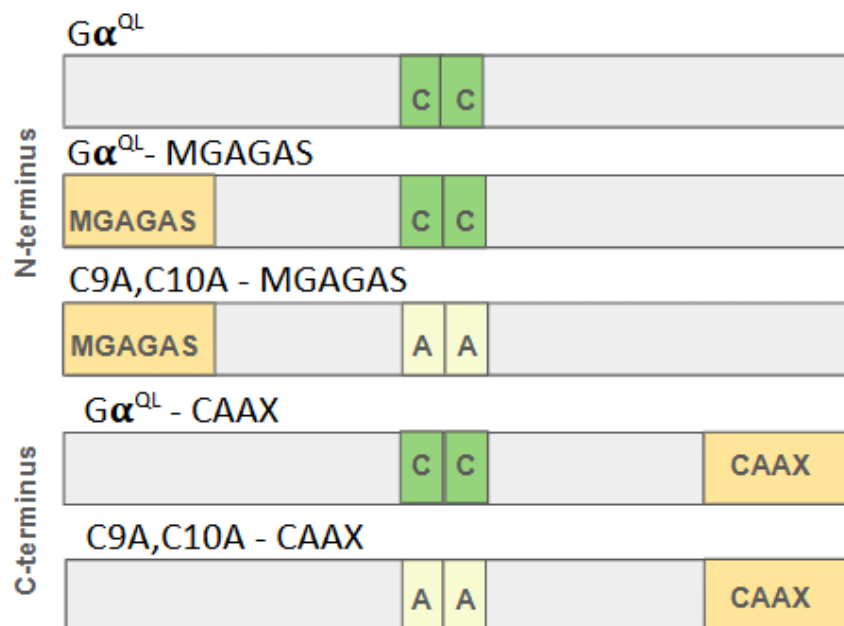


Figure 5. Sequence comparison of $G\alpha_q$ -QL and C9A,C10A mutants containing either a myristoylation motif to the N-terminus, or a CAAX motif to the C-terminus to investigate signal strength or rescue by alternative lipidation sites. Mutations include constructs: $G\alpha_q$ -QL with either a N-terminal myristoylation motif or C-terminal CAAX motif, and C9A,C10A cysteine knockout with either an N-terminal myristoylation motif or C-terminal CAAX motif.

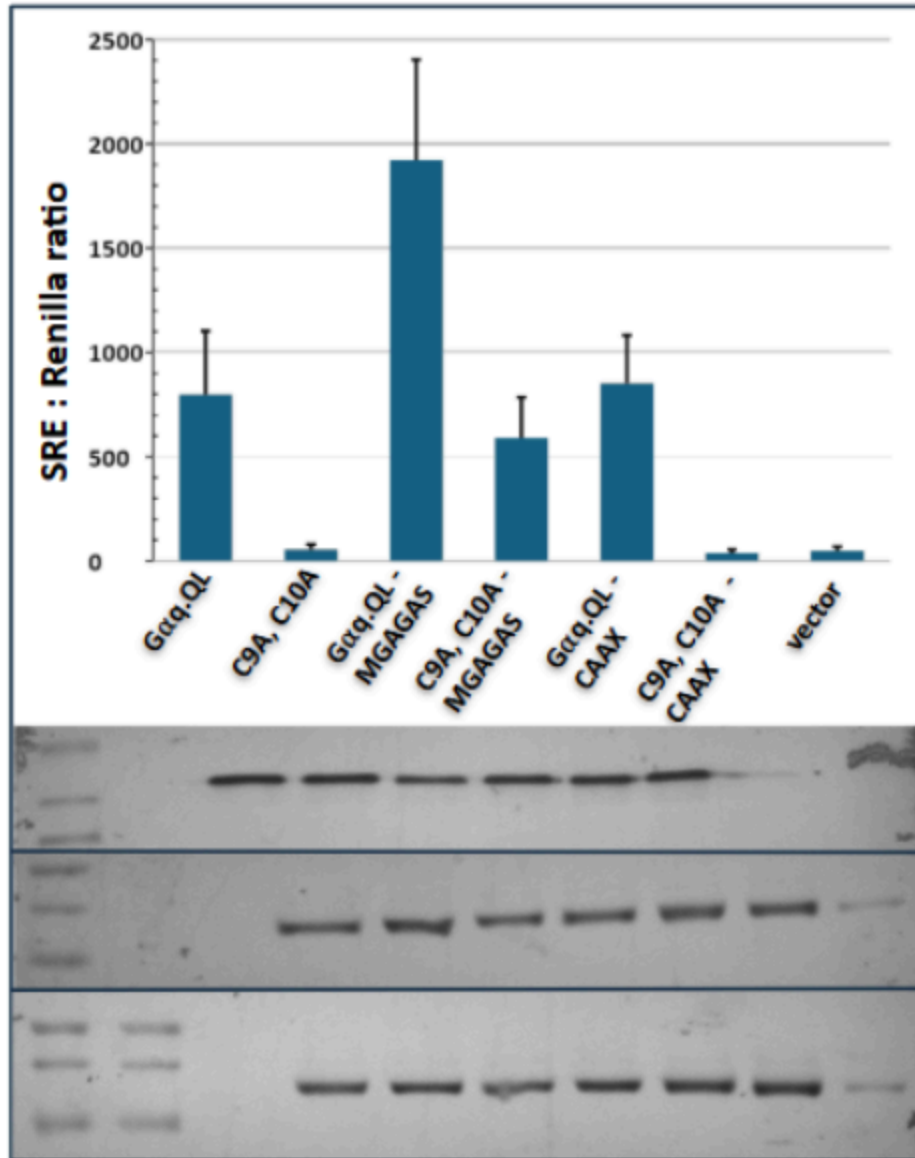


Figure 6. SRE signaling strength of Gαq-QL, pcDNA3.1(+), C9A,C10A as controls, and mutants Gαq-QL-MGAGAS, C9A,C10A-MGAGAS, Gαq-QL-CAAX, C9A,C10A-CAAX as measured by luciferase assay (Methods 2.3). Values are representative of average signaling strength between replicates ± the standard error of the mean. Constructs that contain a myristoylation site (Gαq-QL-MGAGAS, C9A,C10A-MGAGAS) show significant signaling and rescue, while Gαq-QL-CAAX signals closely to Gαq-QL. C9A,C10A-CAAX sees no rescue by the introduction of a C-terminus isoprenyl site. Expression of Gαq/11 protein for all transfected samples was confirmed by western blot analysis. Bands representing Gαq-QL, C9A,C10A, Gαq-QL-MGAGAS, C9A,C10A-MGAGAS, Gαq-QL-CAAX, C9A,C10A-CAAX, and pcDNA3.1(+). Three rounds of replication were performed, with slight band presence seen in pcDNA3.1(+) representing endogenously-encoded Gαq.

Discussion

To investigate the roles of specific contextual amino acids involved in the post-translational palmitoylation necessary for membrane localization at the N-terminus of $G\alpha_q$, a series of constructs were engineered. Experiments were conducted under conditions involving the introduction of negative charges, a phosphomimic, and cysteine knockout mutations, all of which could potentially disrupt palmitoylation to assess the impact of various mutations on signaling and function. Additionally, SRE luminometry assays were performed to measure signaling strength and capability to evaluate the potential for signal rescue through alternative lipid attachment.

SRE signaling and localization were significantly impacted by the single cysteine to alanine substitutions at positions Cys⁹ and Cys¹⁰ in $G\alpha_q$. The complete abolishing of SRE signaling within the C9A,C10A mutant in comparison to the constitutively-active $G\alpha_q$ further indicates that the disruption of the palmitoylation site within the N-terminal region prevents lipid attachment and correct membrane association required for signaling function. In contrast, constructs with phosphomimic mutations flanking the N-terminal cysteines (A8D,L11D, and S12D) did not exhibit the loss of signaling. This difference in outcome, particularly in the mutation of Ser¹² as a common phosphorylation site, suggests that $G\alpha_q$ may utilise a distinct lipidation mechanism or zDHHC protein different from $G\alpha_{12}$, which saw full signal disruption with the introduction of a Ser⁹ to Ala⁹ mutation (Cook, 2022). This $G\alpha_q$ lipidation mechanism may be more akin to $G\alpha_{13}$ lipidation mechanisms, as $G\alpha_{13}$ was similarly unaffected by phosphomimic introduction (Hasan et al., 2023).

Constructs with alternative lipidation sites were generated to further investigate whether the loss of signaling in the C9A,C10A mutant was specifically due to the loss of palmitoylation and to compare the rescues between $G\alpha_q$ -QL and $G\alpha_{12/13}$. Specifically, N-terminal myristoylation (MGAGAS) and C-terminal isoprenylation (CAAX) motifs were introduced into constitutively-active $G\alpha_q$ and the C9A,C10A mutant. The addition of the N-terminal myristoylation site resulted in the upregulation of both $G\alpha_q$ and the rescue of the C9A,C10A mutant, suggesting that the attachment of a myristoyl lipid can compensate for the loss of palmitoylation and restore localisation to the membrane and activation of the SRF pathway. However, the introduction of the isoprenylation motif (CAAX) in the $G\alpha_q$ -QL construct saw minimal signaling difference, with signaling comparable to unmodified $G\alpha_q$ -QL. In contrast, upon measuring the C9A,C10A mutant, the CAAX motif did not restore signaling, indicating that the attachment of an isoprenyl lipid to the C-terminus cannot substitute for the palmitoylation mechanism within $G\alpha_q$. This result is comparable to the behavior of $G\alpha_{13}$ -wt alone, in which the introduced CAAX-motif also fails to signal (Hasan et al., 2022). These results suggest again that $G\alpha_q$ may have specific sequence requirements or mechanisms for membrane localization that cannot be fulfilled by isoprenylation and may suggest that these requirements may be akin to $G\alpha_{13}$ -wt.

Moving forward, the next steps will involve the construction of $G\alpha_q$ - $G\alpha_{13}$ chimeras to further investigate the signaling differences between $G\alpha_q$ and $G\alpha_{13}$. In these experiments, the N-terminal sequences of $G\alpha_q$ -QL and C9AC,10A will be sewn using PCR to the C-terminal sequences of $G\alpha_{13}$ -QL and $G\alpha_{13}$ -wt, either containing a CAAX motif or remaining unmodified. This will allow for an analysis of the signaling

between G α q and G α 13, utilizing the SRE luminometry assay to quantify differences in signal activation under these different conditions, and explore further into G protein unique membrane localisation demands.

Acknowledgment

This research could not have been completed without the continued funding and opportunity provided by the UNCA Undergraduate Research and Creative Activities Program. Thank you to my committee members, Dr. Grosser and Dr. Clark-Hachtel, for their kindness, review, and support. I'd also like to thank the Meigs lab members, past and present: Jack Hendrix for providing the initial oligos for Gq, and Sam Nance and Bailey Cook for their previous research that laid important groundwork. Elizabeth Fangman for her wonderful energy and previous research. And thank you, Gavin Perez and Tasha Taggart, who are finishing this era with me, for all their incredible support and friendship; I could not have done this without them. And thank you to Dr. Meigs for providing such a wonderful opportunity, mentorship, and patience. His dedication to science and passing down his knowledge and passion was an absolute joy. I cannot overstate how much this experience means to me and how much I have learned from it. It has been an absolute delight.

References

1. Annala S, Feng X, Shridhar N, Eryilmaz F, Patt J, Yang J, Pfeil EM, Cervantes-Villagrana RD, Inoue A, Häberlein F, et al. 2019. Direct targeting of gaq and G α 11 oncoproteins in cancer cells. *Sci Signal*. 12(573):eaau5948.
2. Arang N, Gutkind JS. 2020. G protein-coupled receptors and heterotrimeric G proteins as cancer drivers. *FEBS Lett*. 594(24):4201–32.
3. Bhattacharyya R, Wedegaertner PB. 2000. G α 13 requires palmitoylation for plasma membrane localization, rho-dependent signaling, and promotion of p115-RhoGEF membrane binding. *J Biol Chem*. 275(20):14992–9.
4. Chakravorty D, Assmann SM. 2018. G protein subunit phosphorylation as a regulatory mechanism in heterotrimeric G protein signaling in mammals, yeast, and plants. *Biochem J*. 475(21):3331–57.
5. Cook B. 2024. A phosphorylation mimic at the G α 12 N-terminus inhibits palmitoylation and signaling to serum response factor. *UNCA Undergraduate Research Journal*. (Spring 2023).
6. Hasan S, White NF, Tagliatela AC, Durall RT, Brown KM, McDiarmid GR, Meigs TE. 2023. Overexpressed G α 13 activates serum response factor through stoichiometric imbalance with g $\beta\gamma$ and mislocalization to the cytoplasm. *Cell Signal*. 102:110534.

7. Hill CS, Wynne J, Treisman R. 1995. The rho family GTPases RhoA, rac1, and CDC42Hs regulate transcriptional activation by SRF. *Cell*. 81(7):1159–70.
8. Maziarz M, Leyme A, Marivin A, Luebbbers A, Patel PP, Chen Z, Sprang SR, Garcia-Marcos M. 2018. Atypical activation of the G protein gaq by the oncogenic mutation Q209P. *J Biol Chem*. 293(51):19586–99.
9. Qian Y, Zhao Y, Zhang F. 2025. Protein palmitoylation: Biological functions, disease, and therapeutic targets. *MedComm* (2020). 6(3):e70096.
10. Rasheed SAK, Subramanyan LV, Lim WK, Udayappan UK, Wang M, Casey PJ. 2022. The emerging roles of G α 12/13 proteins on the hallmarks of cancer in solid tumors. *Oncogene*. 41(2):147–58.
11. Rasheed SAK, Leong HS, Lakshmanan M, Raju A, Dadlani D, Chong F, Shannon NB, Rajarethinam R, Skanthakumar T, Tan EY, et al. 2018. GNA13 expression promotes drug resistance and tumor-initiating phenotypes in squamous cell cancers. *Oncogene*. 37(10):1340–53.
12. Siehler S. 2009. Regulation of RhoGEF proteins by G12/13-coupled receptors. *Br J Pharmacol*. 158(1):41–9.
13. Suzuki N, Hajicek N, Kozasa T. 2009. Regulation and physiological functions of G12/13-mediated signaling pathways. *Neurosignals*. 17(1):55–70.
14. Veit M, Nürnberg B, Spicher K, Harteneck C, Ponimaskin E, Schultz G, Schmidt MF. 1994. The alpha-subunits of G-proteins G12 and G13 are palmitoylated, but not amidically myristoylated. *FEBS Lett*. 339(1-2):160–4.
15. Wedegaertner PB. 2012. G protein trafficking. *Subcell Biochem*. 63:193–223.
16. Yu OM, Brown JH. 2015. G Protein–Coupled receptor and RhoA-stimulated transcriptional responses: Links to inflammation, differentiation, and cell proliferation. *Mol Pharmacol*. 88(1):171–80.